Sustainable Polymer & Energy

SCIEPublish

Article

Sustainable Lignin-Epoxy Compatibilizer Enables Synergistic Strengthening and Toughening in PBAT/PLA Blends

Xin-Rong Zeng [1], Li-Ming Ye [1], Ling-Ying Shi [2,*] and Ke-Ke Yang [1,*]

[1] The Collaborative Innovation Center for Eco-Friendly and Fire-Safety Polymeric Materials (MoE), National Engineering Laboratory of Eco-Friendly Polymeric Materials (Sichuan), State Key Laboratory of Advanced Polymer Materials, College of Chemistry, Sichuan University, Chengdu 610064, China; 2023222030186@stu.scu.edu.cn (X.-R.Z.); 2025222030233@stu.scu.edu.cn (L.-M.Y.)

[2] State Key Laboratory of Advanced Polymer Materials, College of Polymer Science and Engineering, Sichuan University, Chengdu 610065, China

* Corresponding author. E-mail: shilingying@scu.edu.cn (L.-Y.S.); kkyang@scu.edu.cn (K.-K.Y.)

Received: 12 April 2026; Revised: 8 May 2026; Accepted: 5 June 2026; Available online: 29 June 2026

ABSTRACT: Poly(butylene adipate-co-terephthalate) (PBAT) is a promising biodegradable polyester, but its low strength limits broader application. In principle, blending PBAT with polylactide (PLA) can combine toughness and stiffness, yet severe immiscibility usually leads to poor interfacial adhesion and unsatisfactory overall performance. Here, a bio-based lignin-epoxy composite compatibilizer (E-FL) was developed by premixing ethanol-fractionated lignin (FL) with a protocatechuic-acid-derived epoxy compound and introducing it into PBAT/PLA blends through reactive melt processing. Fractionation enriched lignin fractions with lower molecular weight and higher hydroxyl content, thereby improving reactivity and dispersibility. During melt blending, E-FL promoted interfacial reactions with PBAT and PLA end groups, increased melt torque and molecular weight, refined the dispersed PLA domains, and reduced the T_g gap between the two phases. At an E-FL loading of 3 wt%, the blend exhibited the best balance of performance, with a tensile strength of 36.1 MPa, an elongation at break of 1035%, and a fracture toughness of 238.3 MJ/m^3. This work provides a sustainable strategy for converting lignin into a high-efficiency reactive compatibilizer and offers a practical route to high-performance PBAT-based biodegradable blends.

Keywords: Poly(butylene adipate-co-terephthalate); Polylactide (PLA); Lignin; Bio-based epoxy; Strengthening-toughening synergy

1. Introduction

Growing concern over persistent plastic waste and the transition toward a low-carbon materials economy have accelerated the development of biodegradable polymers as alternatives to conventional petroleum-based plastics [1]. Among them, poly(butylene adipate-co-terephthalate) (PBAT) has attracted significant attention because of its excellent flexibility, processability, and compostability. Nevertheless,

© 2026 The authors. This is an open access article under the Creative Commons Attribution 4.0 International License (https://creativecommons.org/licenses/by/4.0/).

the relatively low modulus and tensile strength of PBAT restricts its use in applications that require higher mechanical integrity [2,3].

Polylactide (PLA), a representative bio-based polyester derived from renewable resources, exhibits high strength and stiffness and has been widely used to enhance PBAT. In principle, blending PBAT with PLA provides a simple and scalable route to combine the ductility of PBAT with the rigidity of PLA [4,5]. In practice, however, the large differences in polarity, chain architecture, and melt rheology between PBAT and PLA lead to poor thermodynamic compatibility. As a result, conventional physical blending generally produces coarse phase-separated morphologies, weak interfacial adhesion, and a simultaneous loss of strength and ductility [6,7].

Reactive compatibilization is one of the most effective approaches for overcoming the intrinsic immiscibility of polyester blends [8]. By introducing multifunctional reactive species during melt processing, interfacial copolymers or branched structures can be generated in situ, thereby reducing interfacial tension, suppressing droplet coalescence, and improving load transfer across the two phases [9–12]. Epoxy or isocyanate chemistries with high reactivity toward polyester end groups have been considered as effective reactive compatibilizers for PBAT/PLA blends, however, most commercialized epoxy are petroleum-derived products [13–17]. Bio-based epoxy compounds derived from unsaturated fatty acids have been explored, but their relatively low epoxy functionality often limits compatibilization efficiency [18]. In contrast, aromatic bio-based epoxies derived from protocatechuic-acid-type structures possess both higher epoxy activity and rigid benzene rings, which may contribute to reinforcement in addition to interfacial coupling [19].

Lignin is the most abundant natural aromatic polymer and represents an underutilized renewable feedstock for advanced materials [20]. Its rigid aromatic framework can enhance stiffness, while its abundant phenolic and aliphatic hydroxyl groups provide versatile reactive sites. However, the direct use of industrial lignin in polymer blends is often hindered by its broad molecular-weight distribution, complex structure, and poor dispersibility [21,22]. Fractionation offers an effective way to isolate lignin fractions with lower molecular weight and higher functional-group density, which are more suitable for reactive processing [23–25]. If such activated lignin is coupled with a reactive bio-based epoxy component, a composite compatibilizer may be obtained that simultaneously delivers renewable content, interfacial reactivity, and structural reinforcement.

In this work, we report a facile strategy to fabricate a PBAT/PLA blend with a good trade-off between strength and toughness (as shown in Figure 1). Ethanol-fractionated lignin (FL) with high hydroxyl content was first premixed with a bio-based aromatic epoxy compound (BioE) to construct a lignin-epoxy composite compatibilizer (E-FL), then it was introduced into PBAT/PLA blends via reactive melt blending with desirable processability. The effects of E-FL loading on blend formation, molecular structure, phase morphology, thermal transitions, dynamic mechanical behavior, and tensile properties were systematically investigated. The structure-property relationship was established by linking interfacial reaction, dispersed-phase refinement, and strengthening-toughening synergy. This study provides a sustainable route for upgrading lignin into a functional compatibilizer high-performance PBAT-based biodegradable blends.

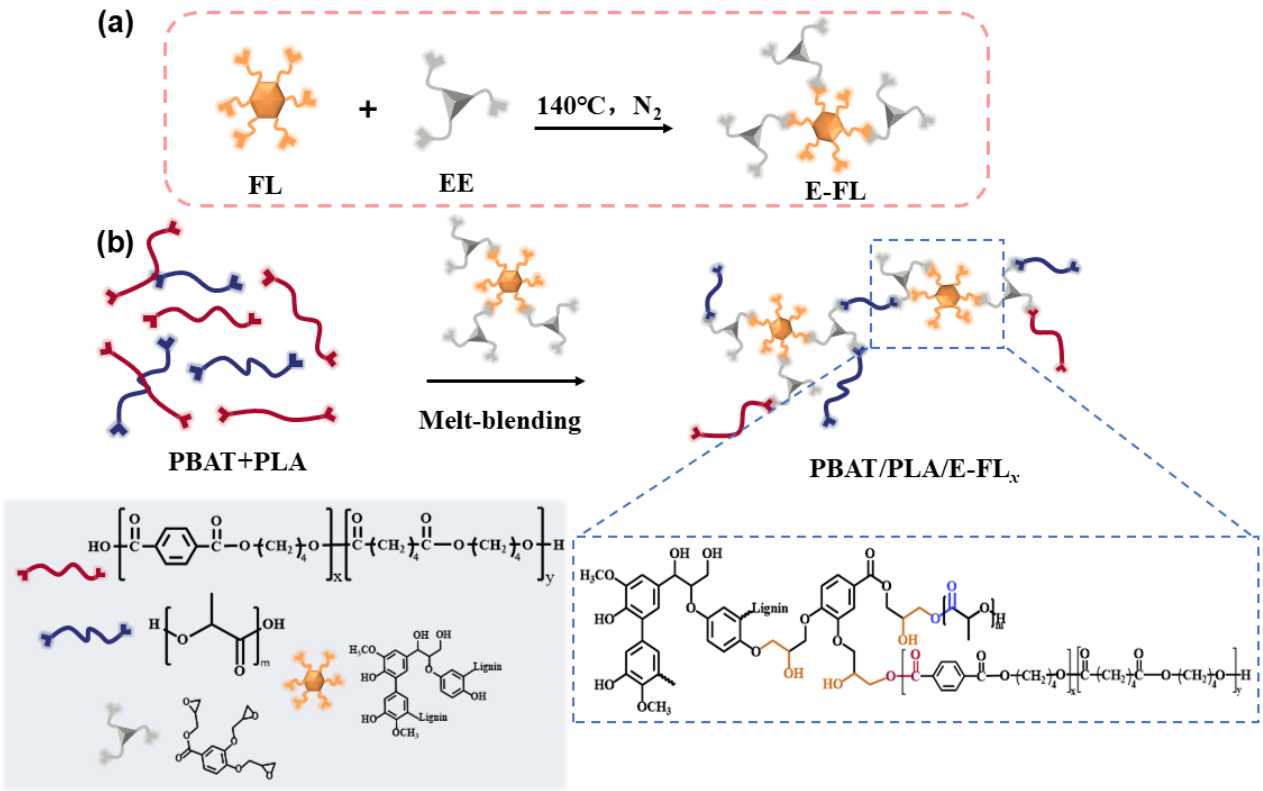


Figure 1. Schematic illustration of (**a**) the preparation of E-FL and (**b**) the synthetic route for PBAT/PLA/E-FL$_x$ composites.

2. Materials and Methods

2.1. Materials

PBAT (A400MF) was supplied by Kingfa Sci. & Tech. Co., Ltd. (Guangzhou, China). PLA (4032D) was purchased from NatureWorks LLC (Plymouth, MN, USA). Alkaline lignin (M_n = 2100 g/mol, particle size: 0.2–20 μm) was obtained from Shanghai Changfa New Materials Co., Ltd. (Shanghai, China). The bio-based epoxy compound derived from protocatechuic acid with epoxy equivalent weight (EEW) of 136, denoted "BioE", was provided by Xinyuxiang New Materials Technology Co., Ltd. (Chengdu, China). Absolute ethanol was purchased from Chengdu Kelong Chemical Co., Ltd. (Chengdu, China). All reagents were used as received.

2.2. Fractionation of Low-Molecular-Weight Lignin (FL)

Low-molecular-weight lignin was extracted from industrial alkaline lignin by solid-liquid extraction with absolute ethanol. Briefly, alkaline lignin (100 g) was dispersed in absolute ethanol (500 mL) and mechanically stirred for 4 h. After filtration to remove insoluble residues, the filtrate was concentrated to approximately 100 mL at 50 °C using rotary evaporation, transferred to an evaporating dish, and allowed to stand in a fume hood for 48 h. The resulting material was then vacuum-dried at 55 °C for 72 h to yield the ethanol-soluble lignin fraction (FL), which was ground into powder before use. The extraction yield was approximately 35%.

2.3. Preparation of the Lignin-Epoxy Composite Compatibilizer (E-FL)

FL was premixed with the bio-based epoxy compound prior to melt blending. Under argon protection, approximately 15 g of BioE was placed in a round-bottom flask and heated to 140 °C until a flowable viscous liquid was obtained. FL (5 g) was then added, and the mixture was stirred for 10 min until it lost

tackiness. After cooling to room temperature, the resulting lignin-epoxy composite compatibilizer was collected and designated E-FL.

2.4. Preparation of PBAT/PLA/E-FLx Blends

A Haake torque rheometer was used as the *in situ* reactive blending reactor. PBAT and PLA were dried in a vacuum oven at 60 °C for 12 h before processing. The PBAT/PLA mass ratio was fixed at 70/30. A series of PBAT/PLA/E-FL$_x$ blends was prepared (see detailed feed ratios in Table S1), where x denotes the E-FL content relative to the total blend mass (0.5, 1, 3, 5, and 7 wt%). PBAT and PLA pellets were first melt-mixed in the rheometer at 170 °C and 60 rpm, after which E-FL was added, and reactive blending was continued for 10 min. The molten blends were removed, cooled, and granulated. A PBAT/PLA blend without E-FL was prepared under the same conditions as the control sample. To ensure identical thermal histories, neat PBAT and neat PLA were also processed under the same melt-processing conditions and were denoted PBAT$_h$ and PLA$_h$, respectively. For film preparation, the granules were compression-molded in a 100 × 100 × 0.5 mm mold using a vacuum hot press at 170 °C. The materials were plasticized for 10 min and then molded under 5 MPa for 2 min to obtain uniform films for subsequent characterization.

2.5. Characterization

Gel permeation chromatography (GPC) was performed to determine molecular weights and molecular-weight distributions. Lignin samples were dissolved in DMF (1–1.5 mg/mL) and measured at room temperature using PMMA standards for calibration. PBAT-, PLA-, and blend-based samples were dissolved in HFIP and analyzed at room temperature with HFIP as the eluent at 1 mL/min. Quantitative 31P NMR spectroscopy was used to determine hydroxyl contents in lignin samples following a phosphitylation procedure based on literature methods [26]. Alcoholic hydroxyl, phenolic hydroxyl, and carboxylic hydroxyl groups were quantified from the corresponding integrated peak areas. Fourier transform infrared (FTIR) spectra were recorded in reflection mode at room temperature over 4000–500 cm^{-1} with a resolution of 4 cm^{-1} and 32 scans.

Differential scanning calorimetry (DSC) was conducted under nitrogen (50 mL/min). Samples (3–5 mg) were first heated to 200 °C at 30 °C/min, held for 2 min to erase thermal history, cooled to −80 °C at 5 °C/min, held for 2 min, and then reheated to 200 °C at 5 °C/min. The crystallinity of PLA in the blends was calculated from the second-heating data using a theoretical melting enthalpy of 93.7 J/g for fully crystalline PLA. Dynamic mechanical analysis (DMA) was carried out from −50 to 100 °C at a heating rate of 3 °C/min, a frequency of 1 Hz, and an amplitude of 20 μm. Field-emission scanning electron microscopy (FESEM) was used to observe cryo-fractured surfaces. Samples were fractured in liquid nitrogen, vacuum-dried at 60 °C for 6 h, sputter-coated with gold, and imaged at an accelerating voltage of 10 kV. Tensile properties were measured using an Instron 5967 universal testing machine equipped with a 500 N load cell. Dumbbell-shaped specimens (50 × 4 × 0.5 mm) were tested at room temperature at a crosshead speed of 50 mm/min. At least five specimens were cut from the hot-pressed films of each sample for testing, and the arithmetic mean and standard deviation were calculated.

3. Results and Discussion

3.1. Preparation of Fractionated Lignin (FL)

Industrial lignin usually exhibits a broad molecular-weight distribution, high structural heterogeneity, and strong intermolecular association, all of which hinder its dispersion and reactivity in polymer matrices. To address these limitations, alkaline lignin was fractionated with absolute ethanol to isolate a lower-molecular-weight fraction enriched in reactive hydroxyl groups (Figure S1). The resulting FL shows a number-average molecular weight of FL 520 g/mol, determined by GPC analysis (Table S2). The hydroxyl

functionalities of Lg and FL were evaluated by ^{31}P NMR, and it revealed that the phenolic hydroxyl content increased from 2.92 to 4.77 mmol/g, and the total hydroxyl content reached 6.04 mmol/g (Table S2). FTIR spectra of FL showed essentially similar characteristic absorption bands with Lg but stronger intensity, including broad O–H stretching near 3400 cm^{-1}, aliphatic C–H stretching around 2936 and 2850 cm^{-1}, C=O stretching near 1705 cm^{-1}, and aromatic skeletal vibrations at 1600, 1510, and 1425 cm^{-1} (Figure S2). It further demonstrates that FL with low-molecular-weight contains higher functional-group densities. The glass-transition temperature (T_g) of lignin decreased significantly from about 150 °C for Lg to 86.78 °C for FL (Figure S3), which should facilitate dispersion and interfacial reaction.

3.2. Fabrication of PBAT/PLA/E-FL$_x$ Blends with E-FL

The E-FL was first prepared by premixing FL with the biobased epoxy compound BioE (derived from protocatechuic acid) at a mass ratio of 1:3 (optimized by pre-experiment) to produce biobased E-FL compatibilizer (Figure 1a). Then it was introduced into the PBAT/PLA melt to effectively couple these two polyester chains at the interface and thereby obtain a series of PBAT/PLA/E-FL$_x$ blends (Figure 1b). Real-time torque monitoring during melt blending provided a direct indication of melt viscosity evolution and the extent of *in situ* reactions.

As shown in Figure 2a, after charging the materials into the mixer, the torque rises rapidly due to the melting resistance and the transient increase in viscosity. With continued mixing, the system becomes progressively more homogeneous, while concurrent chain scission under heat and shear reduces melt viscosity, leading to a gradual decrease in torque. The equilibrium torque of the PBAT/PLA control blend decreased continuously with blending time, indicating progressive thermomechanical degradation under high-temperature, high-shear conditions. After the addition of E-FL, the equilibrium torque increased markedly for all blends except the highest-loading sample. The torque first increased with increasing E-FL content and reached a maximum of about 7.2 N·m at 3 wt% E-FL, then decreased when the compatibilizer content was further increased. This trend indicates that moderate amounts of E-FL effectively promoted interfacial reactions between epoxy groups and the terminal hydroxyl/carboxyl groups of PBAT and PLA, leading to *in situ* formation of branched or grafted structures that enhanced melt strength. At excessive E-FL loadings, however, side reactions, local aggregation, or a dilution/plasticization-like effect likely offset the compatibilization benefit [27].

GPC analysis (Figure 2b) further supports this conclusion. After melt processing, neat PBAT and PLA suffered obvious molecular-weight loss, with M_n decreasing from 6.7 × 10^4 and 12.5 × 10^4 g/mol to 2.3 × 10^4 and 5.8 × 10^4 g/mol, respectively, demonstrating the susceptibility of both polymers to thermomechanical degradation. The PBAT/PLA blend without compatibilizer showed an M_n of only 2.82 × 10^4 g/mol. By contrast, the M_n of the E-FL-containing blends first increased and then decreased with increasing E-FL content, reaching 3.94 × 10^4 g/mol for PBAT/PLA/E-FL$_3$. The good agreement between torque evolution and molecular-weight data confirms that E-FL partially suppressed degradation by promoting chain extension, interfacial coupling, and branching reactions [28].

FTIR spectra provide further molecular-level evidence for the reactive incorporation of E-FL (Figure 2c,d). The characteristic epoxy absorption bands of E-FL at 908 and 843 cm^{-1} disappeared completely in the spectra of the PBAT/PLA/E-FL$_x$ blends, indicating consumption of epoxy groups during melt processing. Meanwhile, the characteristic polyester bands of PBAT and PLA remained visible, showing that the compatibilizer was chemically introduced into the blend rather than simply physically mixed. These results collectively demonstrate that E-FL acted as an effective reactive compatibilizer for PBAT/PLA blends.

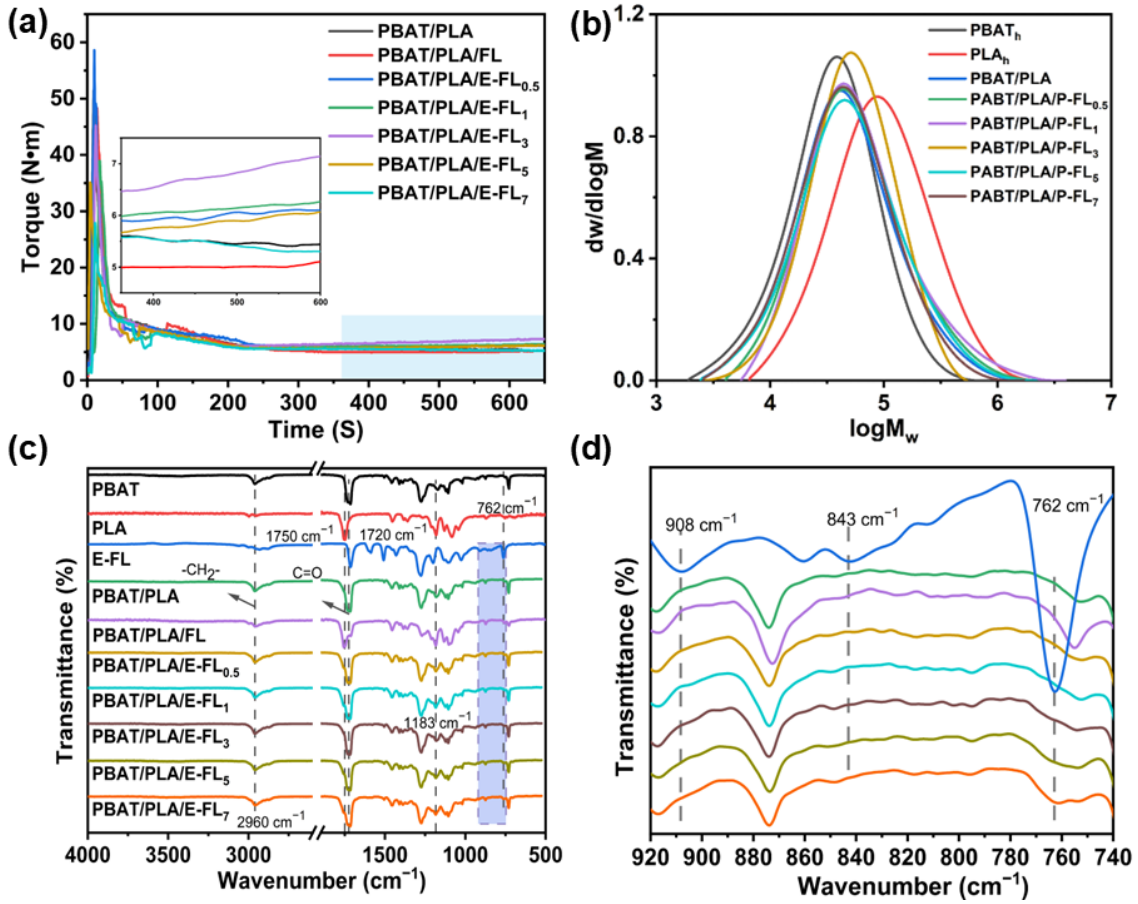


Figure 2. (**a**) Torque-time curves of PBAT/PLA, PBAT/PLA/FL and PBAT/PLA/E-FL$_x$ blends during melt processing; (**b**) molecular-weight distribution curves of the PBAT$_h$, PLA$_h$, PBAT/PLA and E-FL-containing blends; FTIR spectra of raw materials, PBAT/PLA, PBAT/PLA/FL and PBAT/PLA/E-FL$_x$ blends: (**c**) 4000–500 cm^{-1}, (**d**) 920–740 cm^{-1}.

3.3. Morphological Evolution and Phase Refinement

The cryo-fractured surfaces of the blends were observed by FESEM to evaluate phase morphology and interfacial compatibility (Figure 3). Neat PBAT displayed a rough ductile fracture surface, whereas neat PLA showed a smooth brittle fracture surface. The E-FL-free PBAT/PLA blend exhibited a typical sea-island morphology, with PLA dispersed as relatively large droplets in the continuous PBAT matrix, reflecting the strong immiscibility and weak interfacial adhesion between the two polymers [29].

After incorporation of E-FL, the dispersed PLA domains became progressively smaller and more uniformly distributed. The most obvious refinement occurred as the E-FL content increased from 0.5 to 3 wt%, suggesting that the interfacial reaction effectively reduced interfacial tension and suppressed domain coalescence during melt blending. At 5 wt% E-FL, the dispersed domains became even finer, and some regions tended toward a more interconnected morphology. When the E-FL content was further increased to 7 wt%, however, the dispersed phase became slightly coarser again, and a few aggregated regions appeared, implying that excessive compatibilizer induced local enrichment or self-association.

These morphological observations are fully consistent with the chemical evidence discussed above. The reaction of E-FL with both PBAT and PLA at the interface generated interfacial branched or grafted species that anchored the two phases together, promoted droplet breakup under shear, and inhibited recoalescence. Therefore, E-FL significantly improved interfacial compatibility and established the microstructural foundation for improved thermomechanical and mechanical performance.

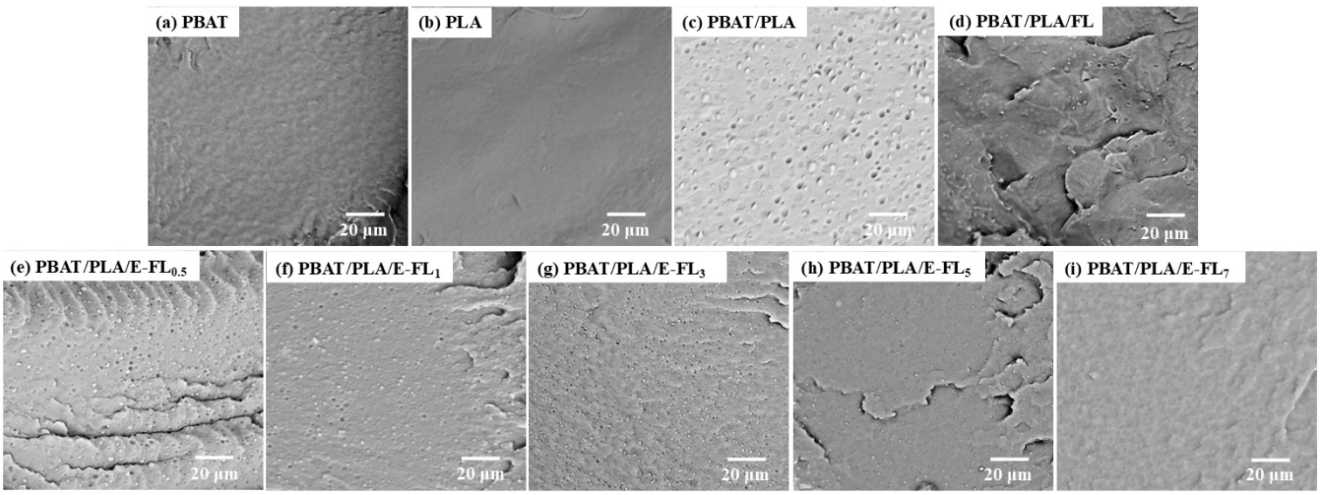


Figure 3. FESEM images of cryo-fractured surfaces: (**a**) PBAT; (**b**) PLA; (**c**) PBAT/PLA; (**d**) PBAT/PLA/FL; (**e**) PBAT/PLA/E-$FL_{0.5}$; (**f**) PBAT/PLA/E-FL_1; (**g**) PBAT/PLA/E-FL_3; (**h**) PBAT/PLA/E-FL_5; and (**i**) PBAT/PLA/E-FL_7.

3.4. Thermal Transitions and Crystallization Behavior

DSC was used to investigate how E-FL affected the thermal transitions and crystallization behavior of the blends (Figure 4a,b), and the crossponding data were summaried in Table S3. Neat PBAT showed a crystallization peak during cooling at 74.4 °C and exhibited T_g and T_m values of −32.5 and 122.1 °C, respectively, during the second heating. Neat PLA did not show an obvious crystallization peak upon cooling at the selected cooling rate because of its slow crystallization kinetics, but displayed a T_g at 59.9 °C, a cold-crystallization peak at 95.4 °C, and a melting peak at 168.7 °C upon reheating.

For the PBAT/PLA control blend, the crystallization temperature of the PBAT phase increased slightly to 77.5 °C, which can be attributed to heterogeneous nucleation induced by the dispersed PLA phase. Once E-FL was introduced, the crystallization peak of PBAT gradually shifted to a lower temperature, reaching 66.9 °C for PBAT/PLA/E-FL_3. This trend indicates that reactive compatibilization and the formation of interfacial branched structures restricted PBAT chain mobility and delayed crystallization. At higher E-FL contents (5 and 7 wt%), $T_{c,PBAT}$ increased slightly again, probably because excess compatibilizer or compatibilizer-rich microdomains provided additional heterogeneous nucleation sites.

The second-heating curves reveal that both PBAT/PLA and PBAT/PLA/E-FL_x samples retained two distinct glass transitions corresponding to the PBAT-rich and PLA-rich phases, confirming that the system remained phase-separated. However, the T_g values of the two phases moved progressively toward each other with increasing E-FL content. The T_g difference decreased from 92.1 °C for the PBAT/PLA blend to 82.0 °C for PBAT/PLA/E-FL_7, indicating enhanced interfacial interaction and partial thermodynamic compatibility [30]. At the same time, the cold-crystallization peak of PLA shifted to a higher temperature, and its crystallinity decreased markedly with increasing E-FL content. For the E-FL_5 and E-FL_7 samples, the PLA cold-crystallization peak nearly disappeared. These changes suggest that chain anchoring at the interface and the steric hindrance of the lignin-containing compatibilizer strongly restricted the rearrangement and crystallization of PLA chains during reheating.

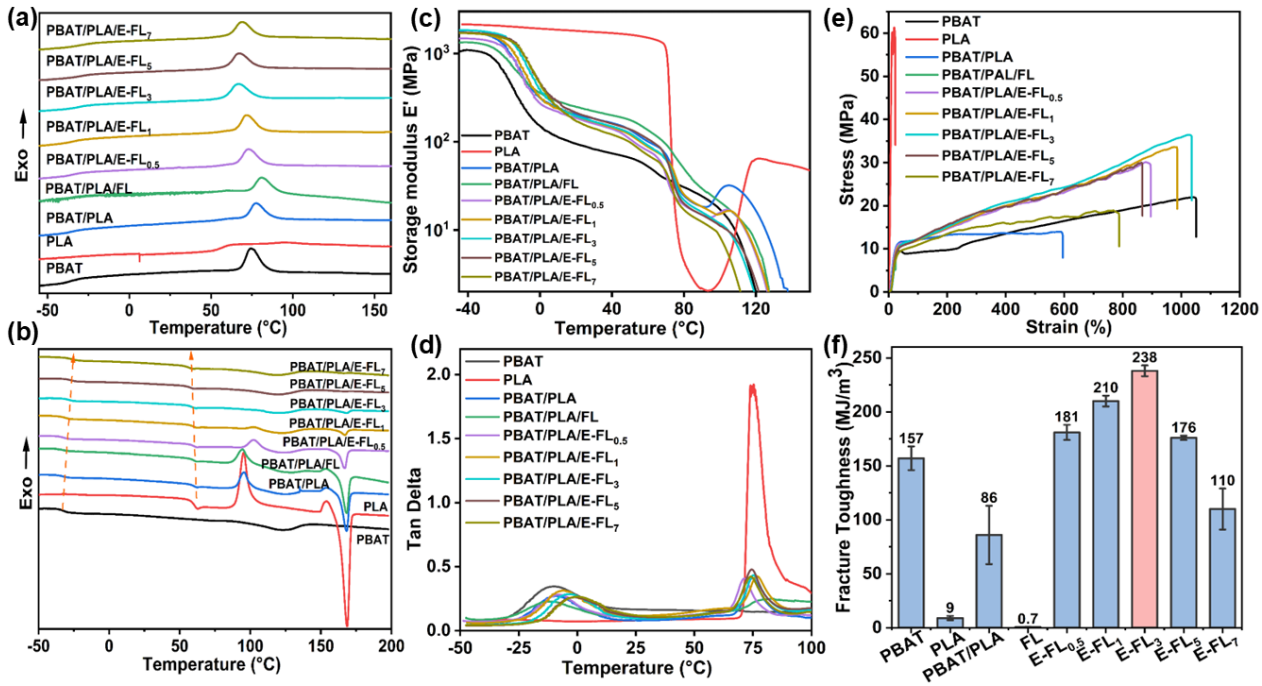


Figure 4. Cooling run (**a**) and the following heating run (**b**) of DSC curves; Storage modulus (**c**) and tan delta (**d**) as a function of temperature recorded by DMA; Tensile stress-strain curves (**e**) and fracture toughness with error bar (**f**) of PBAT, PLA, PBAT/PLA, PBAT/PLA/FL and PBAT/PLA/E-FL$_x$ blends.

3.5. Dynamic Mechanical Behavior

Dynamic mechanical analysis further confirmed the compatibilization effect of E-FL (Figure 4c,d, Table S4). At −50 °C, neat PLA exhibited the highest storage modulus (2.1 GPa) because of its rigid chain structure, whereas neat PBAT showed the lowest value (1.0 GPa). The PBAT/PLA blend displayed an intermediate storage modulus of 1.7 GPa. After incorporation of E-FL, the storage modulus of the blends remained in the range of 1.4–1.8 GPa, with the highest value observed for PBAT/PLA/E-FL$_3$. The moderate increase in stiffness at appropriate E-FL contents can be attributed to improved interfacial load transfer and restricted segmental mobility induced by interfacial reactions.

The tan delta curves of the blends displayed two relaxation peaks corresponding to the glass transitions of PBAT and PLA. With increasing E-FL content, the low-temperature PBAT-related peak shifted gradually toward higher temperature, while the high-temperature PLA-related peak shifted slightly downward. Consequently, the T_g difference measured by DMA decreased continuously from 84.57 °C for the PBAT/PLA blend to 73.99 °C for PBAT/PLA/E-FL$_7$. This trend is in excellent agreement with the DSC results and provides additional evidence that E-FL promoted stronger interfacial interaction between the PBAT and PLA phases.

3.6. Simultaneous Strengthening and Toughening of PBAT/PLA Blends

The tensile properties of neat PBAT and PLA reflect their contrasting mechanical characteristics (Figure 4e, Table S5). PBAT showed excellent ductility, with an elongation at break above 1000%, but relatively low tensile strength (21.8 MPa). PLA, in contrast, exhibited high tensile strength (61.2 MPa) but fractured in a brittle manner at an elongation of only 21%. The control PBAT/PLA blend retained a moderate elongation at break of 586% but suffered a dramatic reduction in tensile strength to 15.3 MPa, which was even lower than that of neat PBAT. This behavior is characteristic of immiscible blends in which weak interfacial adhesion causes stress concentration, interfacial debonding, and premature crack

propagation. Specifically, the dispersed PLA domains embedded in the PBAT matrix act as stress concentrators, where localized stress initiates microcracks and leads to premature failure.

Upon addition of E-FL, both tensile strength and elongation at break increased markedly, demonstrating a rare strengthening-toughening synergy. The optimum performance was achieved at 3 wt% E-FL, where the tensile strength reached 36.1 MPa (even higher than 33.6 MPa, theoretical maximum value of 70/30 PBAT/PLA blend at full compatibility) and the elongation at break reached 1035%. In other words, the compatibilized blend almost fully retained the ductility of neat PBAT while more than doubling the tensile strength of the PBAT/PLA blend. The corresponding fracture toughness increased from 85.6 MJ/m^3 for PBAT/PLA to 238.3 MJ/m^3 for PBAT/PLA/E-FL$_3$ (Figure 4f), representing an improvement of nearly threefold.

When the E-FL load exceeded 3 wt%, the mechanical performance began to deteriorate. This decline is consistent with the reduced torque, lower molecular weight, and slight re-coarsening of phase morphology observed at excessive compatibilizer content. Therefore, the mechanical-property evolution confirms that an appropriate amount of E-FL can effectively reconstruct the PBAT/PLA interface, refine phase morphology, and maximize stress transfer efficiency, whereas excess compatibilizer becomes counterproductive.

4. Conclusions

A sustainable lignin-epoxy reactive compatibilization strategy was developed for PBAT/PLA blends by combining ethanol-fractionated lignin with a bio-based aromatic epoxy compound. Fractionation generated a lignin fraction with lower molecular weight and higher hydroxyl content, while premixing with the bio-based epoxy afforded a highly reactive composite compatibilizer. During reactive melt blending, E-FL participated in interfacial reactions with PBAT and PLA, increased melt torque and molecular weight, refined the PLA dispersed phase, narrowed the T_g difference between the two phases, and suppressed crystallization of both polyester components to different extents. As a result, the interfacial structure and stress-transfer capability of the PBAT/PLA system were markedly improved. The optimum E-FL loading was 3 wt%, at which the blend exhibited a tensile strength of 36.1 MPa, an elongation at break of 1035%, and a fracture toughness of 238.3 MJ/m^3. This work highlights the value of lignin fractionation plus bio-based epoxy coupling as a practical route for transforming renewable aromatic biomass into an efficient reactive compatibilizer, and provides a promising pathway toward high-performance, sustainable PBAT-based biodegradable materials.

Supplementary Materials

The following supporting information can be found at: https://www.sciepublish.com/article/pii/1086, Figure S1: Extraction process for FL; Figure S2: FTIR spectra of Lg and FL; Figure S3: DSC curves of Lg and FL; Table S1: Feed ratios and molecular-weight data; Table S2: Molecular weight and hydroxyl content of Lg and FL; Table S3: DSC data; Table S4: DMA data; Table S5: Mechanical properties.

Statement of the Use of Generative AI and AI-Assisted Technologies in the Writing Process

During the preparation of this manuscript, the authors used ChatGPT in order to refine English expression.

Author Contributions

X.-R.Z.: Investigation, Data curation, Writing—original draft; L.-M.Y.: Formal analysis; L.-Y.S.: Writing—review & editing, Investigation; K.-K.Y.: Conceptualization, Supervision, Writing—review & editing, Investigation.

Ethics Statement

Not applicable.

Informed Consent Statement

Not applicable.

Data Availability Statement

The data presented in this study are available from the corresponding author upon reasonable request.

Funding

National Key Research and Development Program of China (2022YFC2104600/2022YFC2104604), the Fundamental Research Funds for the Central Universities.

Declaration of Competing Interest

The authors declare that they have no known competing financial interests or personal relationships that could have appeared to influence the work reported in this paper.

References

1. Saxena P, Shukla P. A Green Approach to Sustainability: Biodegradable Polymers in Environmental and Energy Applications. *ECS J. Solid State Sci. Technol.* **2025**, *14*, 063005. DOI:10.1149/2162-8777/ade341
2. Wang J, Xu M, Yan J, Guo G, Wang Y, Zhang J, et al. Biodegradable poly(butylene adipate-co-terephthalate) (PBAT) modified by 1,4 cyclohexanedimethanol. *Polymer* **2024**, *308*, 127348. DOI:10.1016/j.polymer.2024.127348
3. Li W, Huang J, Liu W, Qiu X, Lou H, Zheng L. Lignin modified PBAT composites with enhanced strength based on interfacial dynamic bonds. *J. Appl. Polym. Sci.* **2022**, *139*, e52476. DOI:10.1002/app.52476
4. da Silva Pens CJ, Klug TV, Stoll L, Izidoro F, Flores SH, de Oliveira Rios A. Poly (lactic acid) and its improved properties by some modifications for food packaging applications: A review. *Food Packag. Shelf Life* **2024**, *41*, 101230. DOI:10.1016/j.fpsl.2023.101230
5. Venkatesan R, Mayakrishnan V, Alrashed MM, Kim S. Recent Advances in PBAT (Nano) Composite Materials for Food Packaging: A Comprehensive Review. *J. Appl. Polym. Sci.* **2025**, *142*, e57163. DOI:10.1002/app.57163
6. Yeh J, Tsou C, Huang C, Chen K, Wu C, Chai W. Compatible and Crystallization Properties of Poly(lactic acid)/Poly(butylene adipate-*co*-terephthalate) Blends. *J. Appl. Polym. Sci.* **2010**, *116*, 680–687. DOI:10.1002/app.30907
7. Su S. Prediction of the Miscibility of PBAT/PLA Blends. *Polymers* **2021**, *13*, 2339. DOI:10.3390/polym13142339
8. Bao RY, Jiang WR, Liu ZY, Yang W, Xie BH, Yang MB. Balanced strength and ductility improvement of *in situ* crosslinked polylactide/poly(ethylene terephthalate glycol) blends. *RSC Adv.* **2015**, *5*, 34821–34830. DOI:10.1039/c5ra02575c
9. Palsikowski PA, Kuchnier CN, Pinheiro IF, Morales AR. Biodegradation in Soil of PLA/PBAT Blends Compatibilized with Chain Extender. *J. Polym. Environ.* **2018**, *26*, 330–341. DOI:10.1007/s10924-017-0951-3
10. Arruda LC, Magaton M, Bretas RES, Ueki MM. Influence of chain extender on mechanical, thermal and morphological properties of blown films of PLA/PBAT blends. *Polym. Test.* **2015**, *43*, 27–37. DOI:10.1016/j.polymertesting.2015.02.005
11. Freitas ALPDL, Tonini Filho LR, Calvão PS, Souza AMCD. Effect of montmorillonite and chain extender on rheological, morphological and biodegradation behavior of PLA/PBAT blends. *Polym. Test.* **2017**, *62*, 189–195. DOI:10.1016/j.polymertesting.2017.06.030
12. Ma P, Cai X, Zhang Y, Wang S, Dong W, Chen M, et al. *In-situ* compatibilization of poly(lactic acid) and poly(butylene adipate-co-terephthalate) blends by using dicumyl peroxide as a free-radical initiator. *Polym. Degrad. Stab.* **2014**, *102*, 145–151. DOI:10.1016/j.polymdegradstab.2014.01.025
13. Kumar M, Mohanty S, Nayak SK, Rahail Parvaiz M. Effect of glycidyl methacrylate (GMA) on the thermal, mechanical and morphological property of biodegradable PLA/PBAT blend and its nanocomposites. *Bioresour. Technol.* **2010**, *101*, 8406–8415. DOI:10.1016/j.biortech.2010.05.075
14. Dong W, Zou B, Yan Y, Ma P, Chen M. Effect of Chain-Extenders on the Properties and Hydrolytic Degradation Behavior of the Poly(lactide)/Poly(butylene adipate-*co*-terephthalate) Blends. *Int. J. Mol. Sci.* **2013**, *14*, 20189–20203. DOI:10.3390/ijms141020189

15. Nunes EDD, de Souza AG, Rosa DD. Effect of the Joncryl® ADR Compatibilizing Agent in Blends of Poly(butylene adipate-co-terephthalate)/Poly(lactic acid). In Proceedings of the 14th Brazilian Congress on Polymers (CBPol), Aguas de Lindoia, Brazil, 22–26 October 2017.
16. Sun C, Yu Z, Jia L, Zhang X, Zhao Y, Zhang Z. Lightweight and insulation polylactide/poly(butyleneadipate-co-terephthalate) foam with good cushioning performance prepared by supercritical CO_2. *Ind. Crops Prod.* **2025**, *223*, 120067. DOI:10.1016/j.indcrop.2024.120067
17. Mahdipour A, Golshan Ebrahimi N. Ultra-tough polylactic acid/poly(butylene adipate-co-terephthalate) blend for food packaging applications. *J. Elastomers Plast.* **2025**, *57*, 1387–1410. DOI:10.1177/00952443251362821
18. Han Y, Shi J, Mao L, Wang Z, Zhang L. Improvement of Compatibility and Mechanical Performances of PLA/PBAT Composites with Epoxidized Soybean Oil as Compatibilizer. *Ind. Eng. Chem. Res.* **2020**, *59*, 21779–21790. DOI:10.1021/acs.iecr.0c04285
19. Chen X, Hou J, Gu Q, Wang Q, Gao J, Sun J, et al. Corrigendum to "A non-bisphenol-a epoxy resin with high *Tg* derived from the bio-based protocatechuic acid: Synthesis and properties" [Polymer 195 (2020) 122443]. *Polymer* **2020**, *205*, 122726. DOI:10.1016/j.polymer.2020.122726
20. Chio C, Sain M, Qin W. Lignin utilization: A review of lignin depolymerization from various aspects. *Renew. Sustain. Energy Rev.* **2019**, *107*, 232–249. DOI:10.1016/j.rser.2019.03.008
21. Jiang ZH, Argyropoulos DS. Isolation and characterization of residual lignins in kraft pulps. *J. Pulp Pap. Sci.* **1999**, *25*, 25–29. Available online: https://pascal-francis.inist.fr/vibad/index.php?action=getRecordDetail&idt=1715976 (accessed on 1 January 2026)
22. Smit AT, Dezaire T, Riddell LA, Bruijnincx PCA. Reductive Partial Depolymerization of Acetone Organosolv Lignin to Tailor Lignin Molar Mass, Dispersity, and Reactivity for Polymer Applications. *ACS Sustain. Chem. Eng.* **2023**, *11*, 6070–6080. DOI:10.1021/acssuschemeng.3c00617
23. Pang T, Wang G, Sun H, Sui W, Si C. Lignin fractionation: Effective strategy to reduce molecule weight dependent heterogeneity for upgraded lignin valorization. *Ind. Crops Prod.* **2021**, *165*, 113442. DOI:10.1016/j.indcrop.2021.113442
24. Gigli M, Crestini C. Fractionation of industrial lignins: opportunities and challenges. *Green Chem.* **2020**, *22*, 4722–4746. DOI:10.1039/d0gc01606c
25. Sadeghifar H, Wells T, Le RK, Sadeghifar F, Yuan JS, Jonas Ragauskas A. Fractionation of Organosolv Lignin Using Acetone: Water and Properties of the Obtained Fractions. *ACS Sustain. Chem. Eng.* **2017**, *5*, 580–587. DOI:10.1021/acssuschemeng.6b01955
26. Huang J, Wang H, Liu W, Huang J, Yang D, Qiu X, et al. Solvent-free synthesis of high-performance polyurethane elastomer based on low-molecular-weight alkali lignin. *Int. J. Biol. Macromol.* **2023**, *225*, 1505–1516. DOI:10.1016/j.ijbiomac.2022.11.207
27. Guo Y, Zuo X, Xue Y, Zhou Y, Yang Z, Chuang YC, et al. Correction to Enhancing Impact Resistance of Polymer Blends via Self-Assembled Nanoscale Interfacial Structures. *Macromolecules* **2018**, *51*, 3897–3910; Erratum in *Macromolecules* **2019**, *52*, 4785–4785. DOI:10.1021/acs.macromol.9b01000
28. Wang H, Wei B, Gu X, Lin T, Li Y. Determining the optimal molecular architecture for reactive splicing compatibilization: Toward a better understanding of reactive polymer processing. *Polymer* **2020**, *208*, 122948. DOI:10.1016/j.polymer.2020.122948
29. Ayan U, Nouranian S, Majdoub M, Al-Ostaz A, Ucak-Astarlioglu MG, Villacorta BS. Supertoughened Polylactic Acid/Polybutylene Adipate Terephthalate Blends Compatibilized with Ethylene-Methyl Acrylate-Glycidyl Methacrylate: Morphology and Mechanical Properties by the Response Surface Methodology. *Acs Appl. Mater. Interfaces* **2024**, *16*, 26833–26848. DOI:10.1021/acsami.4c06452
30. Zhang L, Goh SH, Lee SY. Miscibility and phase behavior of poly(D,L-lactide)/poly-(*p*-vinylphenol) blends. *J. Appl. Polym. Sci.* **1998**, *70*, 811–816. DOI:10.1002/(SICI)1097-4628(19981024)70:4%3C811::AID-APP22%3E3.0.CO;2-Y